



available at www.sciencedirect.com



journal homepage: www.elsevier.com/locate/jhydrol



Intercomparison of submarine groundwater discharge estimates from a sandy unconfined aquifer

Ann E. Mulligan ^{a,*}, Matthew A. Charette ^b

^a Marine Policy Center, MS 41, Woods Hole Oceanographic Institution, 266 Woods Hole Road, Woods Hole, MA 02543, United States

^b Department of Marine Chemistry and Geochemistry, MS 25, Woods Hole Oceanographic Institution, 266 Woods Hole Road, Woods Hole, MA 02543, United States

Received 30 July 2005; received in revised form 2 November 2005; accepted 18 November 2005

KEYWORDS

Submarine groundwater discharge;
Coastal aquifer;
Thermal image;
Geochemical tracers;
Radium;
Radon

Summary Recent studies suggest that chemical loading from submarine groundwater discharge (SGD) may rival other major sources such as rivers in many coastal areas. SGD can occur as terrestrially-derived, typically fresh, groundwater discharge, or by seawater circulation through aquifer sediments. Because both terrestrial and recirculated seawater SGD can be significant sources of chemical loading to coastal waters, appropriate methods are needed to properly assess and quantify the rates and distribution of these different inputs. Although many techniques exist to quantify SGD, each method samples different components of SGD (e.g., fresh versus saline discharge) over different temporal and spatial scales. The result is that confusion exists about how to use the different methods. In this study, we investigate the applicability of a variety of techniques for estimating SGD from an unconfined sandy coastal aquifer. Physical methods are first used to understand the spatial variability of discharge. This information is then used with physical and geochemical data to estimate SGD. Investigative methods include direct measurement via seepage meters, hydrogeologic estimation using Darcy's law, and tracer-based estimates using radon and radium isotopes. At our field site on Cape Cod, Massachusetts, nearshore landward topography appears to exert a significant control on the spatial variability of fresh groundwater discharge, presumably through its effects on evapotranspiration, and hence recharge, rates. The Darcy estimate of fresh SGD ($4.0 \text{ m}^3 \text{ m}^{-1} \text{ d}^{-1}$) is similar to a previous estimate made using a seepage meter transect that spans the seepage face. Radon serves as a valuable estimator of total SGD (fresh plus saline) ($5.6 \text{ m}^3 \text{ m}^{-1} \text{ d}^{-1}$). The difference between the total and fresh SGD estimates is in good agreement with the radium-based SGD

* Corresponding author. Tel.: +1 508 289 2609.

E-mail addresses: amulligan@whoi.edu (A.E. Mulligan), mcharette@whoi.edu (M.A. Charette).

estimate ($0.56 \text{ m}^3 \text{ m}^{-1} \text{ d}^{-1}$), which primarily measures saline circulation through coastal sediments. Thus, we conclude that the hydrogeologic estimate and radon and radium techniques are complimentary for estimating different components of total SGD at our field site.

© 2005 Elsevier B.V. All rights reserved.

Introduction

The importance of submarine groundwater discharge (SGD) as a source of dissolved solids to coastal waters has become increasingly recognized. Recent studies suggest that SGD-derived chemical loading may rival other major sources such as rivers in many coastal areas (Moore, 1996; Bugna et al., 1996; Kim et al., 2003). Although groundwater flow in most coastal areas occurs as slow diffuse flow, it can be a significant source of dissolved solids because, when compared with surface waters, solute concentrations are often several orders of magnitude more enriched in groundwater (Testa et al., 2002). In estuaries and embayments, SGD often represents a major source of nutrients, which can have considerable ecological effects (Krest et al., 2000; Charette et al., 2001). For example, nitrogen loading into coastal environments can result in eutrophication, which can lead to decreased oxygen content, fish kills, and shifts in the dominant flora (Valiela et al., 1992; Slomp and Van Cappellen, 2004).

Fresh submarine groundwater discharge will occur whenever an aquifer is hydraulically connected with the sea and the water table is above sea level. The driving force behind this process is the hydraulic gradient from the upland region of a watershed to the surface water discharge location at the coast. At the land–sea boundary, seawater flows into aquifer sediments under the force of gravity and thus a complex dynamic flow regime is established as fresh and saline groundwater of different densities interact (Li et al., 1999; Li and Jiao, 2003). Several forcing mechanisms, such as waves, tides, dispersive circulation (Taniguchi et al., 2002; Burnett et al., 2003), and changes in upland recharge (Michael et al., 2005), affect the rate of fluid flow for both fresh and saline groundwater and are ultimately important in controlling the submarine discharge of both fluids.

Groundwater discharging to coastal waters can have salinity that spans a large range and it is therefore important to establish a definition of SGD. Here, we define SGD as any fluid that flows from the sediments into coastal surface water and is comprised of two endmembers: meteoric, typically fresh, water and recirculating seawater. We therefore use the terms fresh SGD and saline SGD to distinguish these sources of fluid and brackish SGD to mean a mixture of the fresh and saline endmembers.

Many studies have focused on methods to quantify SGD, either through point measurements (e.g., Bokuniewicz, 1980; Michael et al., 2003), hydrogeologic models (e.g., Smith and Zawadzki, 2003; Destouni and Prieto, 2003), or by using geochemical tracers that provide a spatially integrated estimate of total flux (e.g., Moore, 1996; Cable et al., 1996; Gramling et al., 2003). However, each of these approaches provide estimates that vary in both the temporal and spatial scales of integration. In order to better understand these inherent differences, intercomparison experiments have been conducted in which different tech-

niques are used to estimate SGD at the same time and place (Burnett et al., 2003). Such experiments are vital for identifying reliable field methods and determining a suite of techniques that are effective across a variety of geologic settings.

The goals of this study were to investigate spatial variability of submarine groundwater discharge from an unconfined sandy coastal aquifer and to perform an intercomparison experiment in which we compare SGD estimates using a variety of techniques sampling at approximately the same time. In particular, we present and compare physical and geochemical data that are used to estimate SGD, including direct measurement via seepage meters, hydrogeologic estimation using Darcy's law, and tracer-based estimates using radon and radium isotopes. The sampling plan was designed in part based on patterns observed in an aerial thermal infrared image of the field site at Waquoit Bay, Cape Cod, Massachusetts, which defines the spatial variability of discharge. At this particular site, near-shore landward topography appears to exert a significant control on the spatial variability ($O(10 \text{ m})$) of fresh groundwater discharge, presumably through its effects on evapotranspiration, and therefore recharge, rates.

Study area: Waquoit Bay, Massachusetts

The field site for this work is located at the northern end of Waquoit Bay, on Cape Cod, Massachusetts (Fig. 1). We first describe regional geologic and hydrogeologic conditions on Cape Cod and then discuss specifics for the Waquoit Bay area.

Regional geology and hydrogeology

Cape Cod was built primarily from glacial processes and outwash plains, terminal moraines, ice-contact deposits, and kettle holes are the predominant landforms (Oldale and Barlow, 1986). On the east–west arm of Cape Cod, known as the Upper Cape, outwash plains of sand and gravel dominate the surficial geology although terminal moraines are present along the western and northern margins.

Fine-grained sediments up to 45 m thick and proposed to be of glaciolacustrine origin lie below the outwash plains (Koteff and Cotton, 1962; Masterson et al., 1997a; Mulligan and Uchupi, 2004). The southern extent of these clay, silt, and very-fine sand deposits is unknown because of limited sampling along the southern coast of Cape Cod and within Nantucket Sound. The glacial lake in which these sediments were deposited may have extended across Nantucket Sound (Masterson et al., 1997a) or may have had its southern terminus along the south shore of Cape Cod (Mulligan and Uchupi, 2004), however, there are insufficient data to distinguish between these two possibilities (Uchupi and Mulligan, in press).

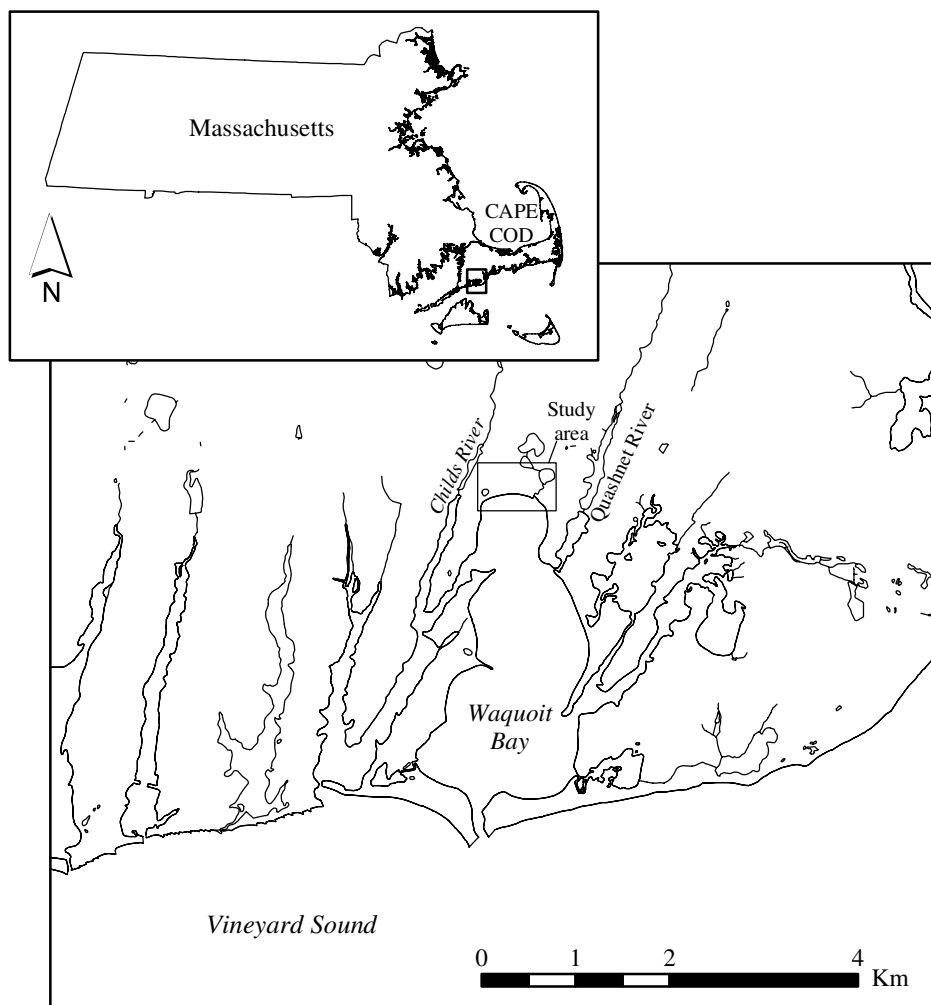


Figure 1 Location map of Waquoit Bay, on Cape Cod, MA, USA.

Because of the highly permeable soils on Cape Cod, groundwater recharge is relatively high, surface runoff is relatively low and streams and rivers are fed primarily by groundwater seepage (Cambareri and Eichner, 1998). Precipitation on the Upper Cape averages $\sim 114 \text{ cm y}^{-1}$ (Walter and Whealan, 2004) and is relatively constant through the year. Half of the measured annual precipitation is estimated to become recharge (LeBlanc et al., 1986). Despite the relatively uniform precipitation, the water table far from significant groundwater supply sources shows seasonal variation of up to 1 m, indicating that evapotranspiration is a significant hydrologic process in the warmer months (Michael, 2004).

Groundwater on Cape Cod is unconfined and occurs as a series of six lenses or mounds (Fig. 2). Within each lens, groundwater flows from the center and apex radially outward and toward the coast. The Sagamore lens is the largest and is located in western Cape Cod, where the top of the mound is $\sim 13 \text{ km}$ north of our study site. Here, the water table ranges from an elevation of 20 m at the apex of the lens down to sea-level along the coast. Regionally, the hydraulic gradient varies from ~ 0.001 near the top of the lens to 0.006 toward the southern coast (Cambareri and Eichner, 1998).

Geology and hydrogeology of Waquoit Bay

Waquoit Bay is located in the town of Falmouth, Massachusetts (Fig. 1). It is a semi-enclosed estuary that exchanges water with Vineyard Sound to the south. The bay has an average depth of 1 m, an area of $\sim 3 \text{ km}^2$ (Michael et al., 2003), and a tidal range of $\sim 1.1 \text{ m}$ (from data supplied by Weidman and Chapman, 2003, 2004, 2005). Water residence time in the bay is approximately 9 days (Charette et al., 2001).

Fresh water enters Waquoit Bay through one of four pathways: direct precipitation, groundwater discharge, or through either the Childs or Quashnet Rivers (Cambareri and Eichner, 1998). A hydrologic mass-balance estimate using long-term average precipitation for the region suggests that total freshwater input to the bay is $0.82\text{--}0.93 \text{ m}^3 \text{ s}^{-1}$, where direct precipitation accounts for 11% of this input, groundwater discharge delivers 34%, and surface water input accounts for the remaining 55% (Cambareri and Eichner, 1998). Although direct groundwater discharge provides 34% of the freshwater input to the bay, groundwater also accounts for 90% of surface water flow. Hence, over 80% of freshwater input to the bay originates as groundwater.

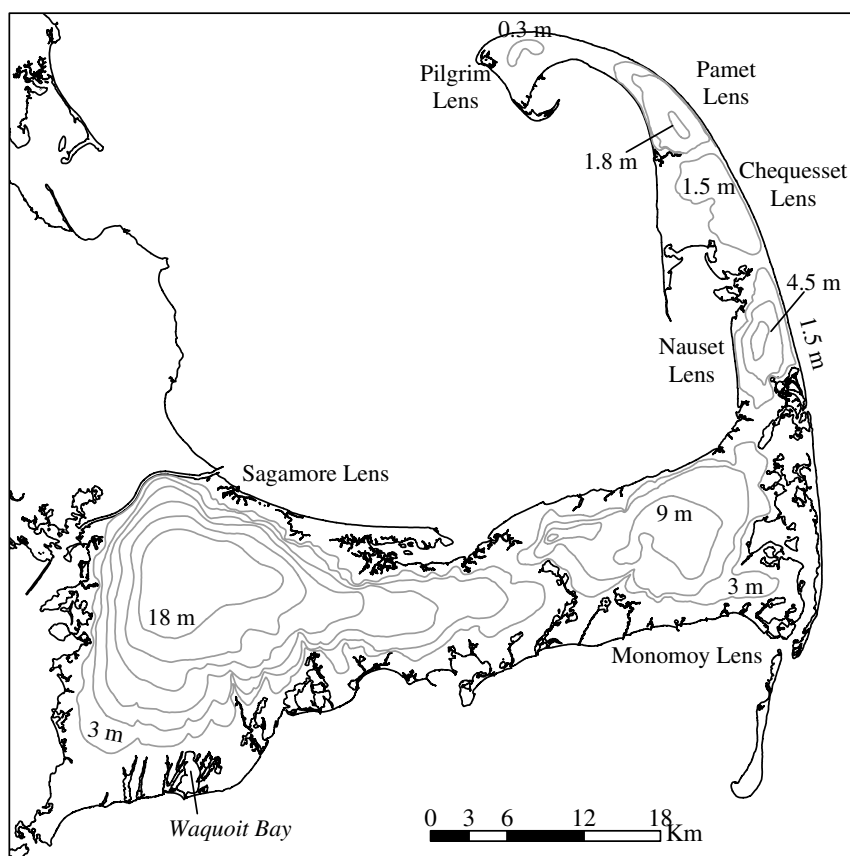


Figure 2 Water table conditions across Cape Cod. Source data was provided by the USGS, the GIS coverage was developed by the Cape Cod Commission, and the GIS datalayer is distributed by the Office of Geographic and Environmental Information (MassGIS), Commonwealth of Massachusetts Executive Office of Environmental Affairs.

Several subwatersheds of Waquoit Bay have been delineated by hydraulic mapping (Valiela et al., 1992; Cambareri and Eichner, 1998) and groundwater flow modeling (Valiela et al., 1997). The head of the bay subwatershed, the region of interest in this study, is $\sim 0.76 \text{ km}^2$ (Cambareri and Eichner, 1998), is triangular in shape, and extends from the head of Waquoit Bay northward $\sim 2 \text{ km}$. Topographically, the head of the bay is characterized by two large bluffs separated by a relict valley, which was likely eroded by groundwater seepage during the last glaciation (Uchupi and Oldale, 1994). The shallow unconfined aquifer is the primary contributor of direct fresh SGD to the head of the bay (Cambareri and Eichner, 1998).

Subsurface soil sampling in the Waquoit Bay area has been relatively sparse and only a few data points exist to shed light on the stratigraphy. Boreholes drilled at the northern end of Waquoit Bay reveal 8–9 m of fine to coarse sand underlain by fine to very fine sand and silt (Cambareri and Eichner, 1998; Michael, 2004). Grain size analysis of several sand samples from the top 2 m at the head of the bay indicates that the shallow sediment consists of $>95\%$ sand and $<5\%$ silt and clay (Charette et al., 2005). The fine grained sand and silt unit below the surficial sand extends to $\sim 45 \text{ m}$ depth, where clay is likely present. During drilling, the top of the clay unit was sampled but the unit's thickness was not determined and remains unknown. Seismic refraction data suggest that bedrock at the head of the bay is

$\sim 100 \text{ m}$ below sea level (Oldale, 1969), but boreholes have not penetrated beyond 45 m. Data from elsewhere on Cape Cod indicate that bedrock ranges from igneous intrusives to metamorphics (Uchupi and Mulligan, in press).

Methods

Several techniques were used to investigate SGD into Waquoit Bay, including airborne thermal imaging, direct measurement via seepage meters, water table mapping, and geochemical tracer analysis. The airborne images and seepage meter measurements were collected during the fall of 2002 and the water table and tracer work were conducted during June–July 2003. Each technique has specific advantages and, when used together, the suite of methods provide valuable insight into the fluid flow regime, including both fresh and saline SGD.

An aerial thermographic survey was conducted by Sensytech Inc. using a Sensytech AA3600 Airborne Multispectral Scanner System on September 7, 2002 between 06 h:00 min and 06 h:30 min local time. The survey was conducted by airplane, with the scanner collecting data through an opening in the belly of the aircraft. Field data collected during summer 2002 indicate that groundwater temperatures in Waquoit Bay were several degrees cooler than bay water, providing a strong thermal contrast. The timing of the survey was chosen to coincide with low tide

during the fortnightly spring tide at Waquoit Bay, when freshwater SGD rates are expected to be maximum (Urish and McKenna, 2004). The thermal image was obtained with a 0.1 °C thermal resolution and a 1 m spatial resolution. Because Waquoit Bay is relatively wide, the entire bay could not be surveyed at the specified spatial resolution in one flight pass over the bay. Instead, the eastern and western halves of the bay were surveyed in two passes.

Seepage meter experiments were conducted using Lee-type manual meters (Lee, 1977) on October 15, 2002, approximately 5 weeks after the thermal image was obtained. These meters are flux chambers with an open end that is placed into the sediments. Fluid inflow or outflow from the sediments is measured by prefilling collection bags with a known volume of water and measuring volumetric changes during the sampling period. Prior to sampling, conditions must be allowed to re-equilibrate after disturbance during meter emplacement. To accomplish this, meters are emplaced at least one day before sampling begins and vent holes on the top of the meters are left open.

Twelve meters were emplaced in a shore parallel transect along the head of the bay and allowed to equilibrate overnight. On the day of the experiment, vent holes on each meter were plugged and plastic bags pre-filled with 1 L of distilled water were attached. Bags were replaced every hour and both the volume and salinity of water in the bags were measured. The experiment took place over half of one tidal cycle, from high tide to low tide.

Hydrologic estimates of fresh SGD were obtained using data from groundwater monitoring wells placed along the head of the bay. Wells installed during this study are constructed of 2.5 cm PVC piping. Each well was installed by hand auguring using 10 cm solid PVC riser as casing; manually installed wells average a depth of about 1.5 m. Each well consists of a 30 cm section of slotted PVC piping threaded to 1.5 m riser sections that extend the well above ground surface. Several pre-existing piezometer nests (see Fig. 5) were also used during this investigation. The screen lengths and diameters of these wells vary, but all are constructed of PVC. Water levels were monitored either by hand using an electronic water level meter (the CCC wells) or using a pressure data logger (all other wells).

Slug tests were conducted at several wells to estimate the horizontal hydraulic conductivity of aquifer sediments. Standard slug-in and slug-out tests were performed and water level response in each well was measured either manually with an electronic water level tape (CCC wells) or with a pressure data logger installed prior to the test and set to collect data every 0.5 s.

The geochemical tracers radium and radon were also used to estimate components of submarine groundwater discharge into Waquoit Bay. Radium and radon are both generated in the uranium–thorium decay series and are therefore ubiquitous in sediments, regardless of composition. They are effective groundwater tracers because they are typically present in elevated concentrations in coastal groundwater relative to the coastal ocean and because they mix conservatively once introduced to surface waters. Hence, relatively simple mass balance models can be used to estimate the flux of groundwater at the coast. Furthermore, radium has four isotopes with half-lives that range

from 3.66 days to 1600 years. The ratios of different radium isotopes can therefore be used to estimate water residence time, which is a key component of the mass balance model.

Baywater (~25 L) and groundwater (~10 L) samples for radium analysis were filtered (1 µm Hytrex II cartridge), collected in cubitainers, and gravity fed slowly (flow rate ~ 1 L min⁻¹) through a column of Mn-impregnated acrylic fibers, which quantitatively extract radium isotopes (Moore and Reid, 1973). Subsamples for salinity analysis were collected in glass bottles from the same samples.

Upon returning to the laboratory, the Mn fibers were partially dried and placed in a delayed coincidence counter for measuring ²²³Ra and ²²⁴Ra (Moore and Arnold, 1996). Samples were recounted after three weeks to correct for supported ²²⁴Ra (via ²²⁸Th). Then, the Mn-fibers were ashed at 820 °C for 16 h, homogenized, and placed in counting vials (Charette et al., 2001). The ash was placed in a well-type gamma spectrometer to measure ²²⁶Ra and ²²⁸Ra activities. Each detector was standardized using NIST-certified standard reference materials (SRMs) sorbed to Mn fibers and prepared in the same geometry as the samples. The short-lived radium isotopes (²²³Ra, ²²⁴Ra) and ²²⁸Ra were decay-corrected to the time of sampling; propagated errors on these measurements were less than 10%.

Groundwater radon samples were collected in 250-mL glass bottles and directly analyzed on a DurrIDGE RAD7 electronic radon monitor using the RAD-H₂O attachment. Activities were decay-corrected to the time of collection. Continuous measurements of ²²²Rn at a single station at the head of Waquoit Bay were obtained using the RAD7 coupled to an air–water equilibrator as described by Burnett and Dulaiova (2003). The instrument recorded the ²²²Rn activity of surface water every 30 min for ~3 days. Tidal height was monitored with a YSI 600 series CTD.

Results

Spatial and tidal variation in SGD

Airborne thermal imagery was obtained between 6:00 and 6:30 am on September 7, 2002. Prior to collecting the images, several data loggers were placed midway into the water column around the head of the bay and in groundwater monitoring wells to provide in situ groundtruthing of water temperatures, to record the tidal signal, and to measure SGD. In situ data confirm that low tide occurred at 6:30 am (Fig. 3) and that peak spring tide occurred on September 6. Weather conditions at flight time were 13–14 °C air temperature, clear skies, and wind of ~1.1 m/s from the north-west (Weidman et al., 2003). Air temperature did not fall below 13 °C during the 22 h prior to data collection. At the time of the overflight, surface water temperatures ranged from 19.5 to 21.5 °C while groundwater temperature was 13 °C. An in situ automated seep meter in place during the imaging (Fig. 3) confirms the presence of submarine groundwater discharge (Sholkovitz et al., 2003).

The two thermal images with 1 m spatial resolution were tiled using GIS and a USGS topographic map as a base map. Several locations at roads, ponds, shorelines, and buildings on each image were tied in to the georeferenced topographic map and the images were spatially transformed

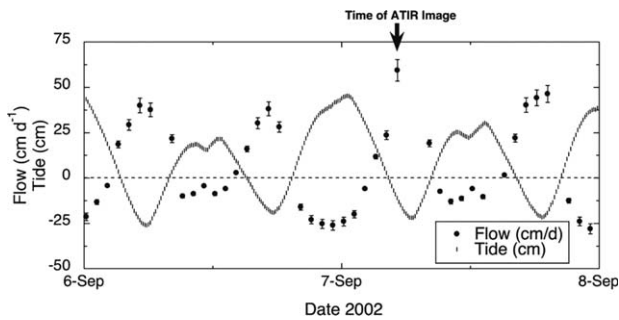


Figure 3 Tidal data at the head of Waquoit Bay for September 6–7, 2002. Peak spring tide occurred on the morning of September 6. On September 7, low tide occurred at 6:30 am. The black circles indicate fluid flow across the sediment–water interface measured by an automated seep meter (see Fig. 5 for location). Image modified from Sholkovitz et al. (2003).

and tiled. In order to highlight the thermal regime in the surface water, the raster data were binned and the range of interest (13–21 °C) was stretched so that differences in water temperatures are clearly visible. The resulting image for Waquoit Bay is shown in Figs. 4 and 5. The location where the images overlap is apparent over the land portion of the survey, where temperatures varied slightly from one flight line to the next. The eastern line was surveyed first

and the vegetation is seen to be slightly cooler than in the later flight line to the west. Despite the thermal differences in the vegetation across the two images, it is clear from road intersections that the images are aligned correctly. Importantly, the surface temperatures in the bay appear to be consistent across the two images.

The thermal image shows a non-uniform temperature distribution along the head of the bay, where surface temperatures vary from 14 to 20 °C. Water temperatures along the beach face range from 13.5 to 14.5 °C. At the inlet between the bay and Vineyard Sound, surface water temperatures vary between 19 and 20 °C while they are a slightly warmer 19.5–20.7 °C 1 km offshore in the Sound (not shown).

The thermal image reveals evidence of diffuse SGD across the head of the bay. In addition, zones of low temperature (~14 °C) are located ~20 m offshore in the central-eastern portion of the head of the bay and about 30 m offshore in the western portion (Fig. 4). Both of these areas are disconnected from the beachface – warmer water is present between the cool water and the beach. Note that both plumes of cooler surface water are offshore of topographic highs (Fig. 4). The cooler plumes are fairly well defined and imply that mixing between SGD and the surface water was sufficiently small that less dense plumes of low salinity cooler water were maintained some distance into the bay. The in situ temperature data indicate that mid-col-

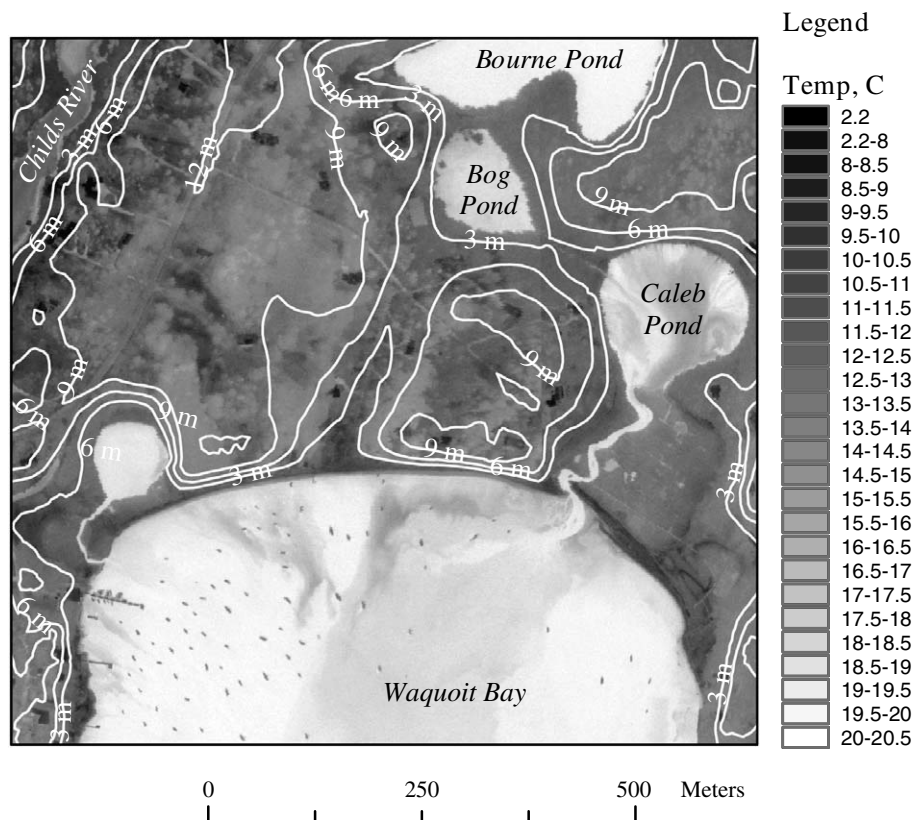


Figure 4 Thermal image of the head of Waquoit Bay. The grey scale indicates surface temperatures. Topographic contours are superimposed on the image with a contour interval of 3 m. Dark spots in the bay are boats. The contour datalayer was provided by the Office of Geographic and Environmental Information (MassGIS), Commonwealth of Massachusetts Executive Office of Environmental Affairs.

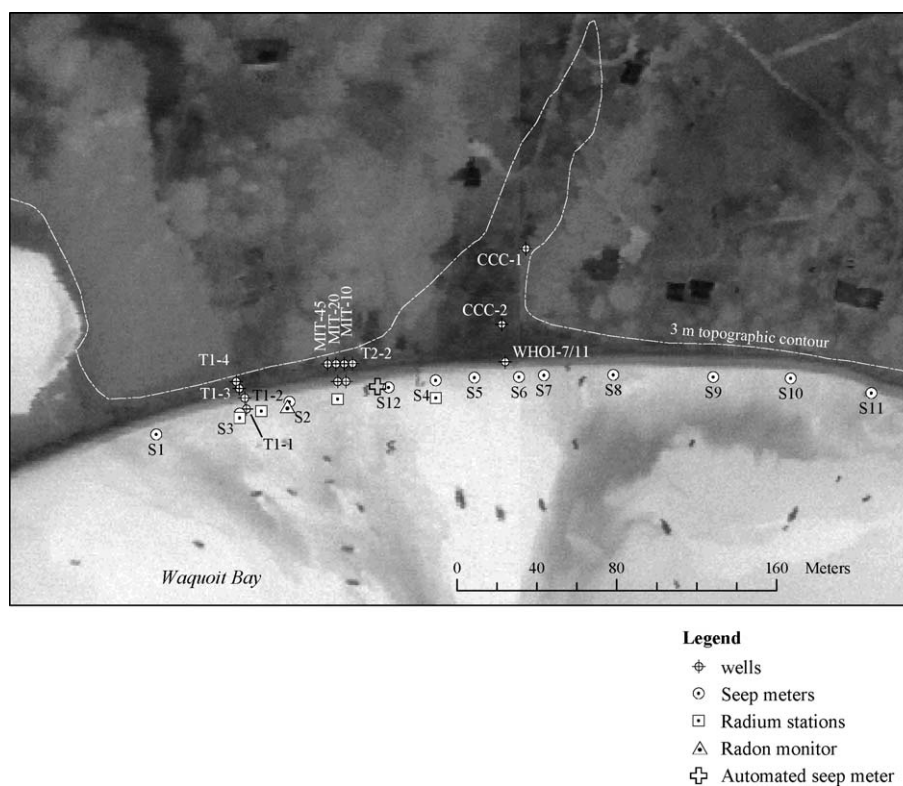


Figure 5 Locations of seep meters, piezometers, the automated seep meter, and radon and radium stations at the head of the bay. Piezometers labeled T#-# were installed during this investigation; all others were preexisting. The temperature scale for the thermal image is shown in Fig. 4.

um Waquoit Bay water was $\sim 20^{\circ}\text{C}$, so the cooler SGD plumes are most likely maintained as a thin surface layer.

Although the hydrology in the nearby ponds was not a focus of this research, it is clear from the thermal image that Caleb Pond has a considerable groundwater input. This is not surprising because most ponds on Cape Cod are considered to be in direct hydraulic connection with the groundwater system. More surprising is the lack of apparent groundwater input to Bourne Pond, only part of which is shown in Fig. 4. One possible explanation for the apparent lack of groundwater input is that low permeability sediment lines Bourne Pond, thereby reducing groundwater discharge. A second possibility is that mixing between groundwater discharge and surface water is sufficiently quick as to mask any thermal signal. This seems unlikely because the groundwater discharge signature elsewhere is quite strong. A third possibility is that Bourne Pond is a losing pond and supplies water to the aquifer. This also seems unlikely because the elevation of the pond is approximately the same as the elevation in Bog and Caleb Ponds (Fig. 4). The likely explanation is that water in Bourne Pond is fresh, the cool groundwater has a higher density than the warmer surface water, and the groundwater is stratified at depth. Conversely, surface water in Caleb Pond, and possibly Bog Pond, likely have high enough salinity that fresh groundwater rises to the surface, imparting a strong thermal signal.

Following receipt of the thermal image, seep meters were deployed along the head of the bay to obtain direct SGD measurements (Fig. 5). Results reveal fairly low seepage rates ($5\text{--}10\text{ cm d}^{-1}$) across the head of the bay during high tide (Fig. 6).

Seepage rates increased with the falling tide, reaching maximums near low tide. Low tide seepage rates varied from $\sim 10\text{ cm d}^{-1}$ at location 4 in mid-head of the bay up to $\sim 40\text{ cm d}^{-1}$ at location 1 along the western margin. In general, low tide seepage rates were highest in the west and east bay and lowest in the mid bay, consistent with the discharge pattern revealed by the thermal image. This spatial pattern is also maintained in the average seepage rates (Fig. 7). Unfortunately, salinity measurements of the seepage fluid during our experiment are anomalously high and therefore unreliable, but data from Michael et al. (2003) indicate that SGD in the region of our experiment is predominately saline.

Although our salinity data from the seepage meters cannot be used to estimate the salinity of discharging water, it does point to a potential unwanted exchange between fluid in the collector bag and fluid in the meter. Presumably fresh water originally in the bag was displaced by more saline water from the meter headspace, resulting in erroneous salinity measurements. Density differences should have prevented such exchange, but the data suggest otherwise.

Variability revealed in water table monitoring

Hydraulic head along the head of the bay was determined using a series of single- and multi-level piezometers that span the area in front of the western bluff and the valley. One transect of piezometers, referred to as the CCC transect and located within the valley, consists of three sets of multi-level wells. Two additional transects are located shoreward of the western bluff within the Waquoit Bay National Estuarine Research Reserve (Fig. 5).

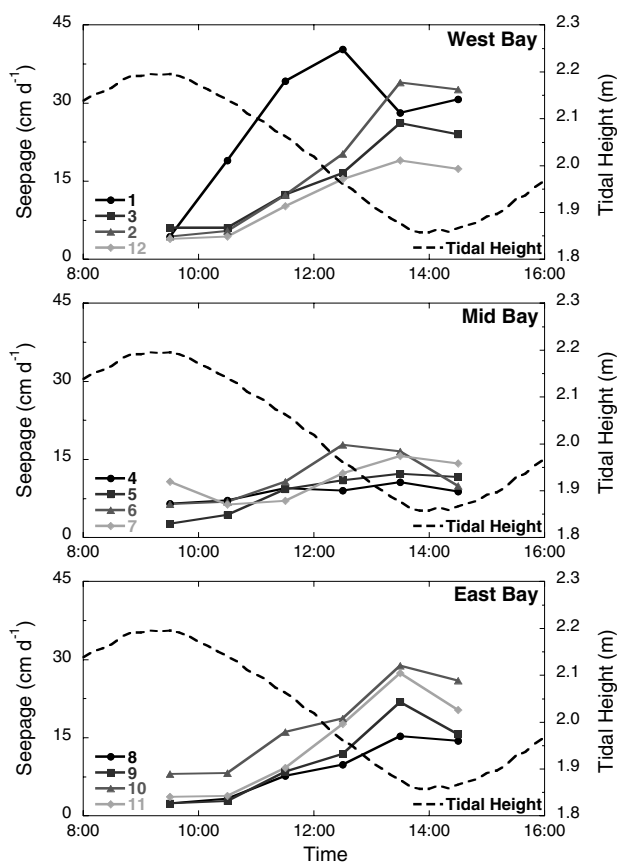


Figure 6 Seep meter data from October 15, 2002. Meter locations are shown in Fig. 5. The scale for the tidal data is plotted on the right-hand axis.

Hydraulic head data reveals that the hydraulic gradient across the head of the bay is not uniform (Fig. 7). At low tide, the gradient between T1-4 and T1-3 at the base of the western bluff is $\sim 0.022 \text{ m m}^{-1}$ ($0.082 \text{ m}/3.75 \text{ m}$) while between wells CCC-1 and CCC-2 in the valley the gradient is 0.004 m m^{-1} ($0.134 \text{ m}/36.4 \text{ m}$). At high tide, these gradients decrease to 0.015 and 0.002 m m^{-1} , respectively.

Significant vertical gradients between groundwater above and below 9 m depth (the contact between sand and finer grained material) indicates upward flow from the locally confined aquifer. Vertical gradients observed in the MIT-45/20 well nest (see Fig. 5 for location) are 0.025 – 0.035 m m^{-1} whereas gradients are approximately half these values at CCC-1.

SGD estimates using hydrogeologic and geochemical techniques

Hydrogeologic estimate

In addition to hydraulic gradients, the horizontal hydraulic conductivity of aquifer sediments is needed to estimate groundwater flow rates. Therefore, both falling and rising head slug tests were conducted at several site wells. Conductivity values calculated from slug tests in the CCC wells are an order of magnitude lower than values calculated from tests in other wells yet there is no apparent geologic explanation for these lower values. It is likely that the con-

struction method of these piezometer nests, in which seven piezometers were tightly bundled in one borehole, restricts flow below that of the natural formation. Therefore, only hydraulic conductivity values from the remaining wells were used in this analysis. Data from the remaining wells reveals hydraulic conductivity values ranging from 32 to 150 m d^{-1} in the surficial aquifer with a geometric mean of 52 m d^{-1} . These values fall within the expected range for clean sands (Freeze and Cherry, 1979) and are consistent with permeameter measurements of 43 – 54 m d^{-1} made using drill cuttings (Michael, 2004) and with values reported for similar lithology elsewhere on the Cape of 45 – 85 m d^{-1} (Masterson et al., 1997b). A slug test in the fine-grained material at MIT-45, which is screened 12 m below ground, reveals a two order of magnitude reduction in hydraulic conductivity.

Groundwater flow rates calculated using Darcy's law, hydraulic gradient data, and the geometric mean of measured hydraulic conductivity reveal nearshore horizontal groundwater velocities averaging 15 cm d^{-1} below the valley and 96 cm d^{-1} below the bluffs. Using the range of measured hydraulic conductivities, the velocities could range from 59 to 278 cm d^{-1} below the bluffs to 9 – 43 cm d^{-1} below the valley. As the freshwater approaches the coastline and the saltwater wedge forces freshwater flow through a smaller flow area, these velocities are expected to increase.

In order to compare our results with those from other investigators, who have estimated volumetric freshwater flux, the cross-sectional area of flow must be determined. Others have assumed a 610 m shoreline (Cambareri and Eichner, 1998; Michael et al., 2003), which stretches from the outlet of Caleb Pond in the east to the unnamed pond in the west (Fig. 4). Head measurements in the multi-level wells indicate that horizontal flow occurs in the unconfined aquifer, while significant vertical gradients lead to upward leakage through the fine-grained unit at 9 m. Vertical hydraulic conductivity in fine-grained material is most likely one to two orders of magnitude less than, and certainly no larger than, horizontal hydraulic conductivity. Assuming the measured horizontal conductivity in the fine-grained unit is an upper limit of vertical conductivity and using the measured vertical gradient of 0.035 m m^{-1} , flow through the confining unit is determined to be insignificant relative to horizontal flow. Furthermore, groundwater below the valley is primarily fresh, reaching a salinity of ~ 15 at the sand-silt contact at CCC-2, hence we consider the fine-grained confining unit as the base of flow, resulting in a saturated thickness of 8.5 m in the valley. At the base of the bluffs, the top 4.5 m of the aquifer is fresh and reaches an equal mixture of fresh and seawater about 5.5 m below the water table (Talbot et al., 2003). Hence, we use a flow depth of 5.5 m for estimating the freshwater flux at the bluffs.

Because the thermal image, seep meter, and water table map reveal different discharge zones along the head of the bay, the 610 m shoreline is segmented into low-lying and high elevation regions, where discharge within each region is assumed to be uniform. The bluffs line about 400 m of the shoreline while lower lying areas occupy the remaining 210 m of shoreline. Based on the geometry of the field area, tidally-averaged hydraulic gradients, and the geometric mean hydraulic conductivity, the total freshwater flux into the head of the bay in June 2003 is estimated to be

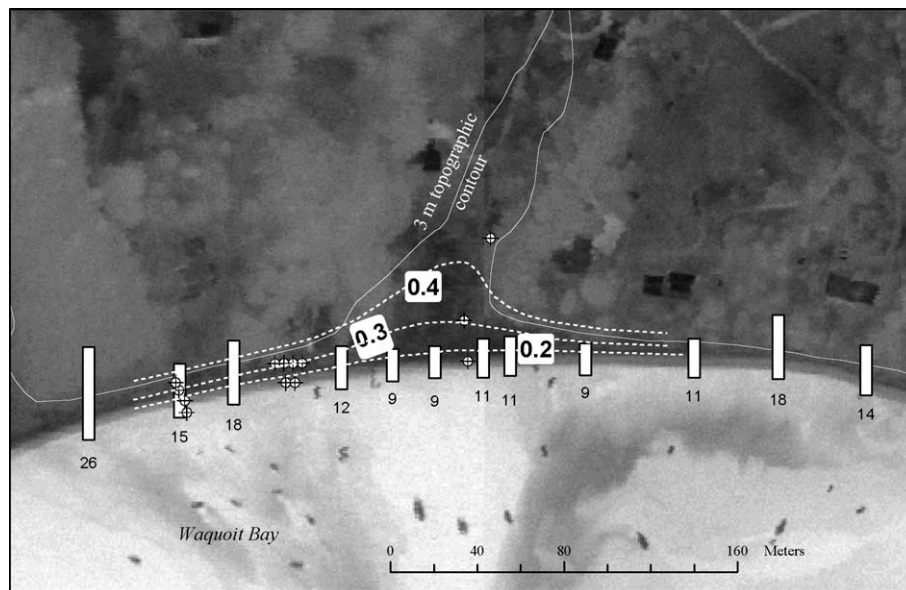


Figure 7 Water table map for June 25, 2003 at low tide. Only data for wells screened toward the top of the unconfined aquifer are shown. Wells screened within and below a low-conductivity zone below 9 m indicate upward leakage of groundwater (data not shown). Head values are in m relative to a fixed datum at the site. The white bars are scaled tidally-averaged seepage rates; numbers below the bars are the seepage rates in cm d^{-1} .

$0.025 \text{ m}^3 \text{ s}^{-1}$ in front of the bluffs and $0.003 \text{ m}^3 \text{ s}^{-1}$ in front of the low-lying areas, for a total of $0.028 \text{ m}^3 \text{ s}^{-1}$ across the shoreline.

Geochemical tracers

Radon

During the same time period that the hydrogeologic measurements described above were collected, we conducted a 2.5-day deployment of a continuous radon monitor at the head of the bay. Radon concentrations in surface water ranged from 1 to 13 dpm L^{-1} and while the lowest values typically occurred at high tide, the peak Rn values often lagged the low tide by 1 or 2 h (Fig. 8a). Groundwater ^{222}Rn activities ranged from 190 to 5900 dpm L^{-1} , with the higher values typically observed at higher salinity (Fig. 9a). Using the approach of Burnett and Dulaiova (2003), we converted the radon concentrations in surface water into an SGD flux time series using a non-steady-state mass balance model. Briefly, to determine the Rn flux due to SGD, we converted the Rn concentrations for each 30-min. interval into inventories using water depth, and corrected for loss to the atmosphere (using local wind speed data), decay, and advective flux out of the head of the bay. The net radon flux ($\text{dpm m}^{-2} \text{ d}^{-1}$) was then divided by the average groundwater Rn concentration ($1.6 \times 10^6 \pm 1.4 \times 10^6 \text{ dpm m}^{-3}$; $n = 29$) to yield a SGD time-series with 30-min resolution (Fig. 8b). In general, Rn-derived SGD was related to tidal state, with the highest values occurring at low tide and the lowest values occurring at high tide (Fig. 8b). Rates ranged from 4 to 12 cm d^{-1} , with an average of $8 \pm 2 \text{ cm d}^{-1}$ ($n = 132$) for the ~ 3 day time-series.

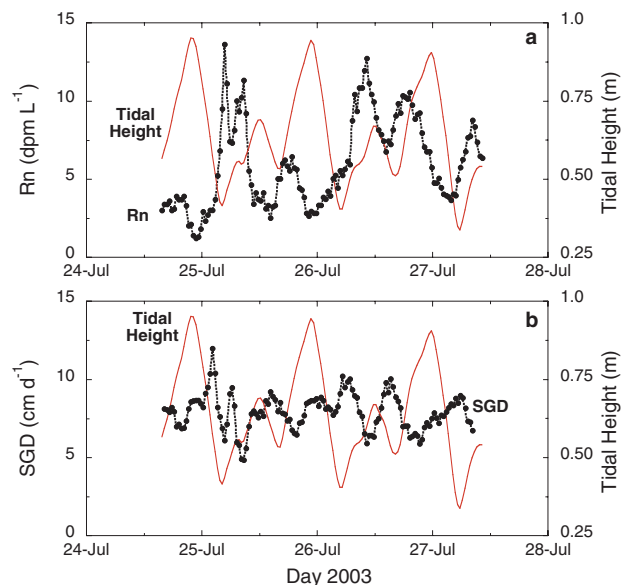


Figure 8 Radon (a) and radon-derived SGD (b) time series at the head of Waquoit Bay during July 2003. The SGD time-series data is plotted as a five-point running average.

Radium

Around the mid-point of the continuous radon monitor deployment, we collected four discrete water samples for radium analysis along a shore parallel transect at the head of the bay (Fig. 5). Radium-226 activities ranged from 13 to 20 $\text{dpm } 100 \text{ L}^{-1}$, with an average of 18 $\text{dpm } 100 \text{ L}^{-1}$.

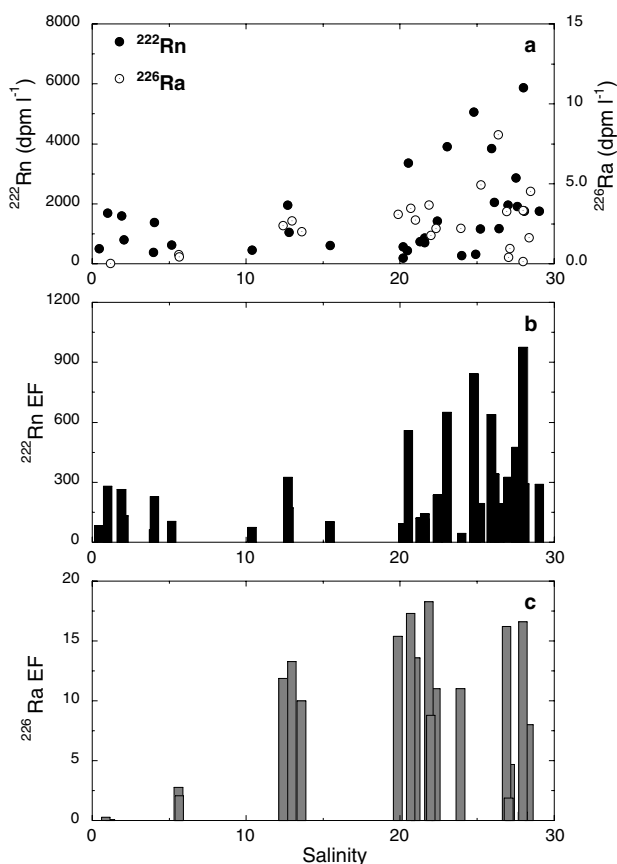


Figure 9 (a) Groundwater radon-222 and radium-226 versus salinity; radon (b) and radium (c) enrichment factors of groundwater relative to average surface water for Waquoit Bay.

Groundwater ^{226}Ra activities ranged from 1.9 to 490 $\text{dpm } 100 \text{ L}^{-1}$ (Fig. 9a); higher values were typically associated with the high salinity groundwater samples. We used the method of Charette et al. (2001) to obtain a ^{226}Ra flux due to SGD, which involves correcting the average Ra inventory for all known sources and sinks other than SGD. Briefly, besides SGD, the major source of Ra to Waquoit Bay is tidal mixing with the coastal ocean (Vineyard Sound $^{226}\text{Ra} = 6 \text{ dpm } 100 \text{ L}^{-1}$; Charette et al., 2001). During this study, we did not evaluate river-derived ^{226}Ra source to the bay, though Charette et al. (2001) determined that it was less than 15% of the total flux. By dividing the net ^{226}Ra inventory ($120 \text{ dpm m}^{-3} \times 1 \text{ m}$ average depth = 120 dpm m^{-2}) by the water residence time of the bay (6.2 days, calculated from the $^{223}\text{Ra}/^{228}\text{Ra}$ activity ratio method; Charette et al., 2001), we estimate a net ^{226}Ra flux due to SGD of $19 \text{ dpm m}^{-2} \text{ d}^{-1}$. We divided this flux by the average groundwater ^{226}Ra concentration of 2400 dpm m^{-3} ($\pm 1900 \text{ dpm m}^{-3}$; $n = 22$) to obtain a radium-derived SGD estimate of 0.8 cm d^{-1} . This value represents a head-of-the bay integrated average of SGD on the time scale of flushing of the bay (~ 1 week). Thus, even though we sampled for Ra only once, we can compare the Ra and Rn-derived SGD estimates, as well as the Darcy estimates, which utilize hydraulic gradient data collected at the same time.

Discussion

Spatial variability in submarine groundwater discharge driven by topography

The thermal image, seep meter data, and water table data all point to spatial variation in nearshore SGD that correlates with onshore topography. The hydraulic gradient shoreward of the western bluff is considerably steeper than it is in the valley. Although gradients are unavailable for the eastern bluff, electromagnetic data from a shore-parallel beach transect just above high tide indicate that salinity conditions in the top 1.5 m are the same adjacent to the bluffs but much more saline in the valley (Belaval, 2003), suggesting that both bluffs probably have similar water table conditions. Therefore, all of the data point to higher fresh SGD rates offshore of the bluffs and lower SGD rates downgradient of low-lying areas. These low-lying areas account for $\sim 35\%$ of the shoreline length but only 11% of the estimated fresh SGD. Total fresh groundwater discharge to the bay is therefore mainly controlled by the amount of water flowing below the high topographic elevations.

In barrier islands along the Florida panhandle, asymmetric freshwater lenses have been observed (Ruppel et al., 2000; Schneider and Kruse, 2003) in which the lens is thickest on the Gulf side and narrows toward the Apalachicola Bay side. Mechanisms responsible for the asymmetry may include some combination of across island variations in hydraulic conductivity and recharge and differences in mean sea level between the gulf and bay sides (Ruppel et al., 2000). Subsequent work reveals a strong correlation between lens thickness and topographic and vegetative differences (Schneider and Kruse, 2003). Although SGD was not measured at these sites, the thicker lens implies a higher water table and steeper gradient at the coast. If hydraulic conductivities are uniform across the narrow islands, then larger fresh SGD occurs along the Gulf side. At Waquoit Bay, there is clearly no difference in mean sea level across the head of the bay and so that mechanism can be discounted. While there may be hydraulic conductivity variations across the head of the bay, the data do not indicate significant horizontal variations in lithology – borehole logs for the CCC and MIT wells all describe a fine to coarse sand in the top 9 m. Although slug tests indicate that the hydraulic conductivity may be an order of magnitude lower at the CCC wells, the well construction method is likely responsible for the low apparent conductivity. These wells were constructed as piezometer nests within a single borehole and the close proximity of other piezometers in the nest likely obstructs flow to each test well, thereby resulting in smaller, and incorrect, estimates of hydraulic conductivity. Furthermore, if groundwater flux through the valley were the same as that through the bluffs, then a lower hydraulic conductivity would require a much steeper gradient, which is not observed. Therefore, the most likely cause of the spatial variation in fresh water SGD rates at Waquoit Bay is the significant topographic features of the valley and bluffs.

The topographic influence on water table elevations likely reflects differences in evapotranspiration (ET) between low-lying areas, where the water table is $< 1 \text{ m}$ deep,

and elevated terrain, where the unsaturated zone is several meters thick. Because groundwater in low-lying areas is closer to the root zone and is more easily taken up by plants (Tarbox and Hutchings, 2001), ET is likely relatively high. Conversely, as water infiltrates into the sandy bluff at Waquoit Bay, it quickly travels below the root zone and is subjected to ET losses for only a short period of time. Hence, we can expect significant differences in net recharge between the bluffs and the valley.

Although one thermal image is not capable of providing sufficient data to estimate SGD rates, the portrayal of spatial variability is useful in guiding field work. Clearly, fluid flow through the low-lying valley is small relative to that below the topographic highs. These different flow rates have important implications for chemical loading estimates and for understanding chemical transformations in the coastal zone. For example, nitrogen loading from fresh groundwater is known to be significant at Waquoit Bay (Valiela et al., 1992; Charette et al., 2001; Talbot et al., 2003) and the vastly different flow rates of water across the head of the bay may affect denitrification rates as SGD passes through nearshore sediments (Capone and Slater, 1990). In another example, Charette and Sholkovitz (2006) found that differences in the depth to the fresh–saline interface across the head of the bay played a role in the contrasting distribution of trace elements in the “subterranean estuary” (Moore, 1999).

The thermal image shows two relatively cold plumes of water beginning ~20 m offshore of both bluffs. Extensive pore water sampling indicates that fresh SGD from the unconfined aquifer is restricted to the nearshore (Michael, 2004) and we therefore think that the plumes visible in the images are not connected to their sources. Instead, these plumes likely originated nearshore and were cut off from their sources by wind or tidal currents. For example, the wind velocity doubled ~30 min before the images were obtained, which probably pushed the existing plumes offshore.

The seep meter data reveal spatial variability in nearshore SGD consistent with the pattern observed from the thermal image, the water table mapping, and seen in previous seep meter studies (see data in Michael, 2004). Unfortunately, our salinity data are unreliable, so we cannot distinguish between two possible explanations for the spatial variability in the seep meter data. If the discharge is brackish, the observed pattern likely reflects the spatial variability of the fresh endmember. However, if the dis-

charge is saline, which is consistent with data from Michael et al. (2003), then the spatial variability in fresh SGD translates into spatial variability in nearshore saline SGD. Such a conclusion is qualitatively consistent with the analytical expression of Li et al. (1999), which describes SGD due to tides as being directly related to the square root of aquifer thickness. At Waquoit Bay, the water table below the bluffs is higher than it is in the valley, resulting in a thicker saturated zone. Therefore, there may be more tidal pumping offshore of the bluffs. Note, however, that if there is a topographic influence on saline circulation, it does not appear to extend far into the bay (see data from Michael, 2004).

A potential problematic exchange of fluid between the seep meter bag and the seep meter was revealed by the salinity data. Resulting predictions for the salinity of porewater are anomalously high, indicating that fresh water in the bag must have been displaced by saline porewater. While there is no reason to believe the volumetric flow rates are erroneous, the salinity data clearly are incorrect and indicate that salinity should not be obtained from fluid in seep meter bags that are prefilled. Short of not pre-filling the seepage meter bags, which can lead to flow bias (Shaw and Prepas, 1989), salinity estimates can be obtained by sampling the shallow porewater adjacent to the seep meter or through the port in the drums while changing the seepage meter bags. In Waquoit Bay, the salinity of porewater changes little over short distances (Michael, 2004), and porewater sampling should therefore produce reliable results.

A hydrogeologic analysis leads to a fresh SGD estimate of $0.028 \text{ m}^3 \text{ s}^{-1}$ across the 610 m head of the bay. This rate assumes both a homogeneous hydraulic conductivity (K) equal to the measured geometric mean K and tidally-averaged hydraulic gradients. The SGD estimate also assumes that the measured hydraulic gradient below the western bluff is representative of the gradient across both bluffs. Similarly, the gradient measured in the valley is assumed to represent all low-lying areas. Although these are significant assumptions, they are consistent with the field data and are therefore considered to be reasonable. Furthermore, the estimated fresh SGD rate is consistent with rates determined using several other methods (Table 1). Michael (2004) estimated fresh discharge of $0.025 \text{ m}^3 \text{ s}^{-1}$ in August 2003 based on seep meter and porewater salinity measurements from the seepage face out to 40 m from shore. Because

Table 1 Estimates of submarine groundwater discharge rates into the head of Waquoit Bay assuming a 610 m shoreline

Source	Fresh SGD (m^3/s)	Saline SGD (m^3/s)	Total SGD (m^3/s)	Method
Cambareri and Eichner (1998)	0.011–0.013 0.012			Recharge estimate Darcy estimate
Michael et al. (2003)	0.001–0.011 ^a		0.047–0.106	Seep meters
Michael (2004)	0.025	0.049	0.074	Seep meters
Charette et al. (2001)		0.43 ^b		Radium isotopes
This study	0.028			Darcy estimate
		0.004		Radium isotopes
			0.035	Radon

^a Seep meter coverage did not extend across entire fresh discharge zone.

^b Estimate is for saline SGD throughout entire bay.

porewater salinity was measured, Michael was able to deconvolute fresh and saline endmember fluxes. Michael et al. (2003) did not sample from the entire seepage face and missed a significant portion of the fresh inflow. Therefore, it is not surprising that their estimate is considerably lower than ours. Cambareri and Eichner (1998) estimated fresh discharge using both a mass-balance approach and Darcy's law. The mass-balance was based on an average recharge rate to the subwatershed, which is assumed to be 50% of long-term average precipitation. The 12 months preceding our 2003 head measurements had considerably higher precipitation than normal, particularly during the spring prior to field work. Hence, our data reflect the temporal component of recharge whereas the Cambareri and Eichner estimate reflects a long-term average. Their discharge estimate calculated using Darcy's law applies the hydraulic gradient from the valley to the entire head of the bay. Our data show that this assumption is not accurate and that the bulk of the freshwater flow occurs offshore of topographic highs.

Intercomparison of methods for quantifying submarine groundwater discharge

A number of geochemical techniques for quantifying SGD have been developed over the past several years (Moore, 1996; Cable et al., 1996; Gramling et al., 2003), but there has been considerable controversy over what component of SGD various techniques are measuring (Younger, 1996; Moore and Church, 1996) and even the reliability of certain methods (Shinn et al., 2002, 2003; Corbett and Cable, 2003). To address these issues, a series of intercalibration experiments for various SGD quantification methods have been conducted (Burnett et al., 2003).

In general, there has been good agreement between geochemical tracers and seepage meters, with the main outlier being estimates based on water balance or Darcy's law calculations. These differences have been attributed to the fact that traditional hydrogeologic methods are quantifying freshwater flow, while the other techniques include a component of recirculated seawater, which happened to be a substantial component of total SGD at the locations studied to date (Burnett et al., 2001).

Thus, a key issue when comparing SGD techniques is the fluid composition that each method is measuring. Whereas the Darcy's law estimate is a measure of the freshwater flux to the head of the bay, the radium and radon methods include a component of recirculated seawater. Because fresh groundwater has a low radium content, it must mix with more saline groundwater along the interface in order to become enriched in Ra isotopes (Abraham et al., 2003; Charette et al., 2003). Thus, any fresh groundwater that bypasses the subterranean estuary will not be quantified by the radium approach. Conversely, ^{222}Rn is a noble gas and groundwater salinity will not control its activity. Furthermore, because of its short half-life, groundwater ^{222}Rn will equilibrate with the sediment-derived ^{226}Ra source after only about three weeks. Hence, unlike Ra, radon should be an ideal tracer of total SGD, regardless of fluid origin or composition.

The groundwater ^{222}Rn and ^{226}Ra concentrations shown in Fig. 9 illustrate these points. Though both ^{222}Rn and ^{226}Ra increase with increasing salinity (Fig. 9a), only ^{222}Rn

is more than two orders of magnitude enriched in groundwater relative to average surface water at all salinities (Fig. 9b). In fact, typical fresh groundwater samples have on average lower ^{226}Ra than surface seawater in Waquoit Bay (Fig. 9c). In contrast, we expect the ^{222}Rn activities to be relatively constant across the fresh–saline interface; while the source of higher activities in the saline zone is unclear, it is possibly due to a greater sediment ^{226}Ra source in offshore sediments (Abraham et al., 2003). The variable activities in both ^{222}Rn and ^{226}Ra across the groundwater salinity gradient (1) illustrates a potential source of uncertainty in using these isotopes as tracers of SGD and (2) raises the issue of the appropriateness of using the average activity to estimate SGD.

There are few, if any, exceptions to the fact that previous studies using radium isotopes or radon as tracers of SGD have reported significant (1–2 orders of magnitude) variability in the endmember tracer concentration (e.g., Moore, 1996; Cable et al., 1996; Krest et al., 2000). Whether or not this leads to uncertainty in the SGD calculation is dependent on whether or not: (1) we have captured the full extent of the true variability in the aquifer of interest; (2) we have properly weighted (in our average) the endmember value to reflect the average concentration of the fluid that is supplying the tracer to the surface water. Regarding (1), a major difference with this work and previous studies is that we have systematically measured the endmember concentrations via a significant number of measurements across the full salinity gradient. Thus, to simply propagate, for example, the standard deviation of the groundwater average through to the SGD estimate would greatly overestimate the true uncertainty of the technique as we have applied it.

Regarding (2), given that flow rates in the fresh portion of the aquifer are likely much faster than in the brackish to saline zone, would it be more appropriate to use a weighted average? One argument against this would be that the greater aerial extent of saline SGD likely outweighs faster flow over a smaller area as with fresh SGD. A better understanding of the spatial distribution of SGD rates would be needed to justify using a weighted average endmember tracer activity in studies such as presented here. However, this results in a circular argument: SGD rates are needed to determine a weighted average SGD rate using radium and radon isotopes. Clearly this is untenable and so we continue to use average groundwater concentrations while recognizing that the tracers provide an excellent qualitative indication of SGD and an uncertain quantitative estimate.

A second key issue in comparing SGD estimation techniques relates to scaling. Whereas the geochemical tracers will give a shoreline or estuary-integrated estimate of SGD, seepage meters and hydrogeologic methods apply where the measurements are conducted and resulting estimates must be scaled up; this disconnect can be overcome by making more point measurements over the area of interest. In our case, the tracer-based SGD estimates are likely including not only discharge along the head of the bay, but SGD that occurs on the eastern and western shores of Waquoit Bay, which can be seen as thermal anomalies in Fig. 4. We will therefore use shoreline fluxes ($\text{m}^3 \text{m}^{-1} \text{d}^{-1}$) in order to compare the Darcy, radon and radium-derived SGD estimates.

For fresh SGD, the volumetric flux estimate of $0.028 \text{ m}^3 \text{ s}^{-1}$ must be divided by the shoreline length

(610 m), which produces an average shore-normal fresh SGD estimate of $4.0 \text{ m}^3 \text{ m}^{-1} \text{ d}^{-1}$. For radium-derived SGD, Michael (2004) observed a measurable ^{226}Ra flux from seepage meters to a distance of 70 m offshore. Thus, the radium estimate of 0.8 cm d^{-1} , when normalized to this seepage face width, becomes $0.56 \text{ m}^3 \text{ m}^{-1} \text{ d}^{-1}$. Assuming the same seepage width, the radon-derived SGD estimate of 8 cm d^{-1} translates to $5.6 \text{ m}^3 \text{ m}^{-1} \text{ d}^{-1}$. The difference between the radon and radium estimates of $\sim 5 \text{ m}^3 \text{ m}^{-1} \text{ d}^{-1}$, agrees quite well with the Darcy estimate and suggests that a substantial portion of the fresh SGD at this location bypasses the subterranean estuary. This observation has significant biogeochemical implications because denitrification may be enhanced during fresh–saline groundwater mixing but minimized in freshwater nitrate plumes that discharge through the seepage face with minimal interaction with saline groundwater (Talbot et al., 2003).

The shoreline fluxes observed here are of similar magnitude to previous intercomparison exercises held in Florida ($3\text{--}35 \text{ m}^3 \text{ m}^{-1} \text{ d}^{-1}$) and Australia ($2\text{--}8 \text{ m}^3 \text{ m}^{-1} \text{ d}^{-1}$) (Burnett et al., 2003). An intercalibration experiment in New York, which was held in a hydrogeologic setting quite similar to Waquoit Bay, produced estimates ranging from $5 \text{ m}^3 \text{ m}^{-1} \text{ d}^{-1}$ (Rn-derived; Dulaiova et al., submitted) to $7.5 \text{ m}^3 \text{ m}^{-1} \text{ d}^{-1}$ (seepage meter; Sholkovitz et al., 2003; assuming a seepage face of 50 m), both in good agreement with our total SGD estimate.

In contrast with our study, past intercalibration experiments at Florida (Burnett et al., 2002) and New York (Dulaiova et al., submitted) found excellent agreement between both radon and radium-based estimates of SGD. What, therefore, can explain why our radium-derived SGD estimate is so low at Waquoit Bay compared with the radon estimate? One possibility is the unusually wet spring that preceded our sampling in June 2003, where water levels in the aquifer reached a near 10-year maximum. When this occurs, the fresh–saline interface is forced in a seaward direction, and the fluid encounters sediments that have been somewhat depleted in Ra-isotopes due to the fact that they have been exposed to seawater for many months/years (Charette et al., 2003). Hence, through this process, the groundwater-derived Ra flux to the bay may have been lower during this time period when compared with average summertime conditions.

Conclusions

The objectives of this study were to examine the spatial variability of submarine groundwater discharge (SGD) along the head of Waquoit Bay and to compare several techniques for estimating fresh and saline SGD. This study demonstrates the utility of aerial thermal images in assessing along-shore variability in fresh groundwater discharge. Though single images are not useful for quantifying SGD, they are quite valuable in guiding field-work such as hydrogeologic and geochemical tracer based studies. The infrared image of the field site aided in planning field-work and in interpreting the hydraulic head data and seepage measurements.

The data reveal that spatial variability in alongshore SGD can be significant. Because shallow sediment on Cape Cod is generally considered to be fairly uniform and homogeneous,

we expected to observe fairly uniform discharge across the head of the bay. The thermal image clearly shows significant discharge offshore of topographic highs and much lower discharge near low-lying areas. The discharge patterns seen in the image are also reflected in the water table and seepage meter data. Topographic influences, which can have significant impact on net recharge, are likely the major driver of spatial variability in fresh SGD at Waquoit Bay. The topographic influence on SGD may extend to nearshore saline SGD patterns, although our salinity data do not allow us to conclude this with certainty.

The salinity data from the seepage meter experiment reveal an exchange of fluid between the collection bag and the meter that is unacceptable for measuring porewater salinity. We therefore recommend that porewater salinity either be measured in sediment adjacent to the meter or through the sampling port on the meter.

The Darcy estimate for average fresh groundwater discharge from the water table aquifer into the head of Waquoit Bay is $0.028 \text{ m}^3 \text{ s}^{-1}$, or $4.0 \text{ m}^3 \text{ m}^{-1} \text{ d}^{-1}$. This value agrees well with a prior estimate calculated from seepage meter measurements (Michael, 2004). The radium-based estimate of SGD, which is most sensitive to brackish and saline discharge, is $0.56 \text{ m}^3 \text{ m}^{-1} \text{ d}^{-1}$. Finally, the radon-based estimate of SGD, which measures total discharge (fresh plus saline), is $5.6 \text{ m}^3 \text{ m}^{-1} \text{ d}^{-1}$. Although each technique measured a different component of groundwater discharge at Waquoit Bay, the resulting discharge estimates are consistent with one another and show that a variety of techniques are needed to understand subsurface flow regimes across the land–sea boundary.

Acknowledgments

The authors thank Dan Abraham, Matt Allen, Craig Herbold, Rachel Hutchinson, Kevin Kroeger, Adam Rago, Ed Sholkovitz, and Jenny Talbot, all from WHOI at one time or another, for their assistance in the field; Chris Weidman, from the Waquoit Bay National Estuarine Research Reserve, for logistical support; and Charlie Harvey and Holly Michael, MIT, for granting access to the MIT wells and for numerous discussions about SGD into Waquoit Bay. We also thank Alain Bourg and an anonymous reviewer for their valuable input, which helped improve the manuscript. This research was supported by a grant from the Coastal Ocean Institute at the Woods Hole Oceanographic Institution (A.E.M./M.A.C.), a National Science Foundation Grant (OCE-0095384; M.A.C.), and a WHOI Coastal Ocean Institute Fellowship (M.A.C.).

References

- Abraham, D.M., Charette, M.A., Allen, M.C., Rago, A., Kroeger, K.D., 2003. Radiochemical estimates of submarine groundwater discharge to Waquoit Bay, Massachusetts. *Biological Bulletin* 205, 246–247.
- Belaval, M., 2003. A geophysical investigation of the subsurface salt/fresh water interface structure, Waquoit Bay, Cape Cod Massachusetts. Masters Thesis, Boston College.
- Bokuniewicz, H.J., 1980. Groundwater seepage into Great South Bay, New York. *Estuarine and Coastal Marine Science* 10, 437–444.

- Bugna, G.C., Chanton, J.P., Cable, J.E., Burnett, W.C., Cable, P.H., 1996. The importance of groundwater discharge to the methane budgets of nearshore and continental shelf waters of the northeastern Gulf of Mexico. *Geochimica et Cosmochimica Acta* 60 (23), 4735–4746.
- Burnett, W.C., Dulaiova, H., 2003. Estimating the dynamics of groundwater input into the coastal zone via continuous radon-222 measurements. *Journal of Environmental Radioactivity* 69, 21–35.
- Burnett, W.C., Taniguchi, M., Oberdorfer, J., 2001. Measurement and significance of the direct discharge of groundwater into the coastal zone. *Journal of Sea Research* 46, 109–116.
- Burnett, W., Chanton, J., Christoff, J., Kontar, E., Krupa, et al., 2002. Assessing methodologies for measuring groundwater discharge to the ocean. *EOS* 83 (11), 122, 123.
- Burnett, W.C., Bokuniewicz, H., Huettel, M., Moore, W.S., Taniguchi, M., 2003. Groundwater and pore water inputs to the coastal zone. *Biogeochemistry* 66, 3–33.
- Cable, J.E., Bunga, G.C., Burnett, W.C., Chanton, J.P., 1996. Application of ^{222}Rn and CH_4 for assessment of groundwater discharge to the coastal ocean. *Limnology and Oceanography* 41, 1347–1353.
- Cambareri, T.C., Eichner, E.M., 1998. Watershed delineation and ground water discharge to a coastal embayment. *Ground Water* 36 (4), 626–634.
- Capone, D.G., Slater, J.M., 1990. Interannual patterns of water table height and groundwater derived nitrate in nearshore sediments. *Biogeochemistry* 10 (3), 277–288.
- Charette, M.A., Sholkovitz, E.R., 2006. Trace element cycling in a subterranean estuary: Part 2. Geochemistry of the pore water. *Geochimica et Cosmochimica Acta* 70, 811–826.
- Charette, M.A., Buesseler, K.O., Andrews, J.E., 2001. Utility of radium isotopes for evaluating the input and transport of groundwater-derived nitrogen to a Cape Cod estuary. *Limnology and Oceanography* 46 (2), 465–470.
- Charette, M.A., Splivallo, R., Herbold, C., Bollinger, M., Moore, W.S., 2003. Salt marsh submarine groundwater discharge as traced by radium isotopes. *Marine Chemistry* 84, 113–121.
- Charette, M.A., Sholkovitz, E.R., Hansel, C., 2005. Trace element cycling in a subterranean estuary: Part 1. Geochemistry of the permeable sediments. *Geochimica et Cosmochimica Acta* 69, 2095–2109.
- Corbett, D.R., Cable, J.E., 2003. Seepage meters and advective transport in coastal environments: Comments on “Seepage meters and Bernoulli’s revenge” by E.A. Shinn, C.D. Reich, T.D. Hickey, 2002. *Estuaries* 25, 126–132. *Estuaries* 26 (5), 1383–1387.
- Destouni, G., Prieto, C., 2003. On the possibility for generic modeling of submarine groundwater discharge. *Biogeochemistry* 66 (1–2), 171–186.
- Dulaiova, H., Burnett, W.C., Chanton, J.P., Moore, W.S., Bokuniewicz, H.J., Charette, M.A., Sholkovitz, E., submitted. Assessment of groundwater discharges into West Neck Bay, New York, via natural tracers. *Continental Shelf Research*.
- Freeze, R.A., Cherry, J.A., 1979. *Groundwater*. Prentice-Hall, Englewood Cliffs, NJ.
- Gramling, C.M., McCorkle, D.C., Mulligan, A.E., Woods, T.L., 2003. A carbon isotope method to quantify groundwater discharge at the land–sea interface. *Limnology and Oceanography* 48 (3), 957–970.
- Kim, G., Lee, K.K., Park, K.S., Hwang, D.W., Yang, H.S., 2003. Large submarine groundwater discharge (SGD) from a volcanic island. *Geophysical Research Letters* 30 (21) (Art. No. 2098).
- Koteff, C., Cotton, J.E., 1962. Preliminary results of recent deep drilling on Cape Cod, Massachusetts. *Science* 137, 34.
- Krest, J.M., Moore, W.S., Gardner, L.R., Morris, J.T., 2000. Marsh nutrient export supplied by groundwater discharge: evidence from radium measurements. *Global Biogeochemical Cycles* 14, 167–176.
- LeBlanc, D.R., Guswa, J.H., Frimpter, M.H., Londquist, C.J., 1986. Groundwater resources of Cape Cod, Massachusetts. US Geological Survey Hydrologic Investigations Atlas HA-692, 4 plates.
- Lee, D.R., 1977. A device for measuring seepage flux in lakes and estuaries. *Limnology and Oceanography* 22 (1), 140–147.
- Li, H.L., Jiao, J.J., 2003. Tide-induced seawater–groundwater circulation in a multi-layered coastal leaky aquifer system. *Journal of Hydrology* 274 (1–4), 211–224.
- Li, L., Barry, D.A., Stagnitti, F., Parlange, J.-Y., 1999. Submarine groundwater discharge and associated chemical input to a coastal sea. *Water Resources Research* 35 (11), 3253–3259.
- Masterson, J.P., Stone, B.D., Walter, D.A., Savoie, J., 1997a. Hydrogeologic framework of western Cape Cod, Massachusetts. United States Geological Survey Hydrologic Investigations Atlas HA-741, 1 sheet.
- Masterson, J.P., Walter, D.A., Savoie, J., 1997b. Use of particle tracking to improve numerical model calibration and to analyze ground-water flow and contaminant migration, Massachusetts Military Reservation, Western Cape Cod, Massachusetts. United States Geological Survey Water Supply Paper 2482.
- Michael, H., 2004. Seasonal dynamics in coastal aquifers: investigation of submarine groundwater discharge through field measurements and numerical models. PhD Dissertation, MIT.
- Michael, H.A., Lubetsky, J.S., Harvey, C.F., 2003. Characterizing submarine groundwater discharge: a seepage meter study in Waquoit Bay, Massachusetts. *Geophysical Research Letters* 30. doi:10.1029/2002GL016000.
- Michael, H.A., Mulligan, A.E., Harvey, C.F., 2005. Seasonal oscillations in water exchange between aquifers and the coastal ocean. *Nature* 436, 1145–1148. doi:10.1038/nature03935.
- Moore, W.S., 1996. Large groundwater inputs to coastal waters revealed by ^{226}Ra enrichments. *Nature* 380, 612–614.
- Moore, W.S., 1999. The subterranean estuary: a reaction zone of ground water and sea water. *Marine Chemistry* 65, 111–125.
- Moore, W.S., Arnold, R., 1996. Measurement of ^{223}Ra and ^{224}Ra in coastal waters using a delayed coincidence counter. *Journal of Geophysical Research* 101, 1321–1329.
- Moore, W.S., Church, T.M., 1996. Submarine groundwater discharge, reply to Younger. *Nature* 382, 122.
- Moore, W.S., Reid, D.F., 1973. Extraction of radium from natural waters using manganese-impregnated acrylic fibers. *Journal of Geophysical Research* 90, 6983–6994.
- Mulligan, A.E., Uchupi, E., 2004. Wisconsinian glacial lake sediments in the subsurface of Cape Cod, Massachusetts. *Northeastern Geology and Environmental Science* 26, 188–201.
- Oldale, R.N., 1969. Seismic investigations on Cape Cod, Martha’s Vineyard, and Nantucket, Massachusetts, and a topographic map of the basement surface from Cape Cod to the Islands. United States Geological Survey Professional Paper 650-B, B122–B127.
- Oldale, R.N., Barlow, R.A., 1986. Geologic map of Cape Cod and the Islands Massachusetts. United States Geological Survey Miscellaneous Investigation Series Map I-1763.
- Ruppel, C., Schultz, G., Kruse, S., 2000. Anomalous fresh water lens morphology on a strip barrier island. *Ground Water* 38 (6), 872–881.
- Schneider, J.C., Kruse, S.E., 2003. A comparison of controls on freshwater lens morphology of small carbonate and siliciclastic islands: examples from barrier islands in Florida, USA. *Journal of Hydrology* 284, 253–269.
- Shaw, R.D., Prepas, E.E., 1989. Anomalous short-term influx of water into seepage meters. *Limnology and Oceanography* 34 (7), 1343–1351.
- Shinn, E.A., Reich, C.D., Hickey, T.D., 2002. Seepage meters and Bernoulli’s revenge. *Estuaries* 25 (1), 126–132.
- Shinn, E.A., Reich, C.D., Hickey, T.D., 2003. Reply to comments by Corbett and Cable on our paper, “Seepage meters and Bernoulli’s revenge. *Estuaries* 26 (5), 1388–1389.

- Sholkovitz, E., Herbold, C., Charette, M., 2003. An automated dye-dilution based seepage meter for the time-series measurement of submarine groundwater discharge. *Limnology and Oceanography: Methods* 1, 16–28.
- Slomp, C.P., Van Cappellen, P., 2004. Nutrient inputs to the coastal ocean through submarine groundwater discharge: controls and potential impact. *Journal of Hydrology* 295 (1–4), 64–86.
- Smith, L., Zawadzki, W., 2003. A hydrogeologic model of submarine groundwater discharge: Florida intercomparison experiment. *Biogeochemistry* 66 (1–2), 95–110.
- Talbot, J.M., Kroeger, K.D., Rago, A., Allen, M.C., Charette, M.A., 2003. Nitrogen flux and speciation through the subterranean estuary of Waquoit Bay, Massachusetts. *Biological Bulletin* 205, 244–245.
- Taniguchi, M., Burnett, W.C., Cable, J.E., Turner, J.V., 2002. Investigation of submarine groundwater discharge. *Hydrological Processes* 16, 2115–2129.
- Tarbox, D.L., Hutchings, W.C., 2001. Topographic influences on the development of freshwater lenses in coastal and island aquifers in lower and middle latitude climatic zones. In: *Proceedings of the World Water and Environmental Resources Congress*. ASCE, Orlando, FL.
- Testa, J.M., Charette, M.A., Sholkovitz, E.R., Allen, M.C., Rago, A., Herbold, C.W., 2002. Dissolved iron cycling in the subterranean estuary of a coastal bay: Waquoit Bay, Massachusetts. *Biological Bulletin* 203, 255–256.
- Uchupi, E., Mulligan, A.E., in press. Late Pleistocene stratigraphy of Upper Cape Cod and Nantucket Sound, Massachusetts, *Marine Geology*.
- Uchupi, E., Oldale, R.N., 1994. Spring sapping origin of enigmatic valleys of Cape Cod and Martha's Vineyard and Nantucket islands. *Geomorphology* 9, 83–95.
- Urish, D.W., McKenna, T.E., 2004. Tidal effects on ground water discharge through a sandy marine beach. *Ground Water* 42 (7), 971–982.
- Valiela, I., Foreman, K., LaMontagne, M., Hersh, D., Costa, J., Peckol, P., DeMeo-Andreson, B., D'Avanzo, C., Babione, M., Sham, C.-H., Brawley, J., Lajtha, K., 1992. Couplings of watersheds and coastal waters: sources and consequences of nutrient enrichment in Waquoit Bay, Massachusetts. *Estuaries* 15 (4), 443–457.
- Valiela, I., Collins, G., Kremer, J., Lajtha, K., Geist, M., Seely, B., Brawley, J., Sham, C.H., 1997. Nitrogen loading from coastal watersheds to receiving estuaries: new method and application. *Ecological Applications* 7 (2), 358–380.
- Walter, D.A., Whealan, A.T., 2004. Simulated water sources and effects of pumping on surface and ground water, Sagamore and Monomoy flow lenses, Cape Cod, Massachusetts. United States Geological Survey Scientific Investigations Report 2004–5181.
- Weidman, C., Chapman, K., 2003. Waquoit Bay National Estuarine Research Reserve Water Quality Metadata, January 2002–December 2002.
- Weidman, C., Chapman, K., 2004. Waquoit Bay National Estuarine Research Reserve Water Quality Metadata, January 2003–December 2003.
- Weidman, C., Chapman, K., 2005. Waquoit Bay National Estuarine Research Reserve Water Quality Metadata, January 2004–December 2004.
- Weidman, C., Chapman, K., Payne, R., 2003. Waquoit Bay National Estuarine Research Reserve Meteorological Metadata, January 2002–December 2002.
- Younger, P.L., 1996. Submarine groundwater discharge. *Nature* 382, 121.